

Effects of Saw Blade Geometry on Oil Palm Frond Cutting

Umesh Ganesh, Zaidi Mohd Ripin, Wan Mohd Amri Wan Mamat Ali, And Mohamad Ikhwan Zaini Ridzwan*

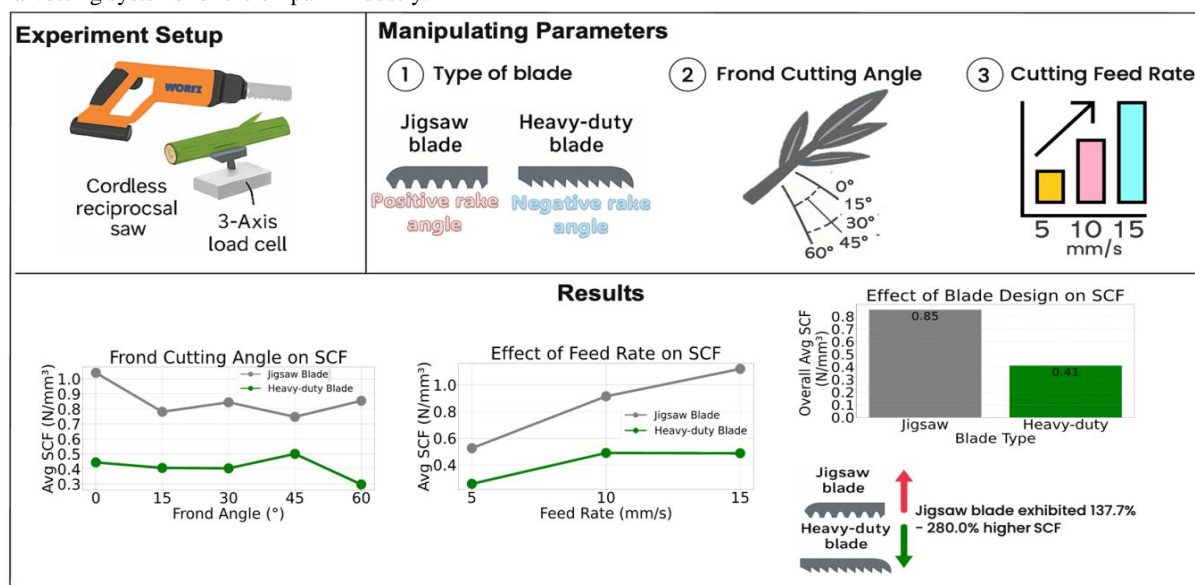
Neurorehabilitation Engineering and Assistance Systems Research, School of Mechanical Engineering, Engineering Campus, Universiti Sains Malaysia, 14300, Nibong Tebal, Penang, Malaysia.

Received 26 Jun 2025

Accepted 31 Jul 2025

Abstract

Harvesting oil palm is heavily reliant on manual effort due to the high cutting force required, especially with traditional sickles featuring narrow wedge angles. Mechanised alternatives, such as reciprocating saws, offer potential to reduce manual efforts. This study investigates the influence of frond cutting angles (0° , 15° , 30° , 45° , 60°), feed rates (5, 10, 15 mm/s), and blade types (Jigsaw blade and heavy-duty pruning blade) on cutting forces using a cordless electric reciprocal saw. Specific Cutting Force (SCF), defined as the cutting force per volume of frond removed per stroke, was found to be higher for the jigsaw blade compared to the heavy-duty blade. At a 0° relative frond cutting angle and 15 mm/s feed rate, the SCF for the jigsaw blade increased from 0.35 N/mm^3 to 1.64 N/mm^3 , while the heavy-duty blade showed a smaller increase from 0.14 N/mm^3 to 0.69 N/mm^3 . The jigsaw blade's performance declines at higher frond angles and feed rates, requiring up to 280% more force than the heavy-duty blade under those conditions. Cutting efficiency, notably at 30° frond cutting angle, the heavy-duty blade was over 250% more efficient than jigsaw blade, highlighting its advantage in high demand cutting conditions. These findings highlight the importance of blade design and cutting conditions in optimizing harvesting efficiency, with mechanized tools like the reciprocal electric saw reducing worker strain and improving productivity. The findings support the use of mechanised tools to reduce physical strain and enhance efficiency and can support the design of advanced robotic or drone-based automated harvesting systems for the oil palm industry.



© 2025 Jordan Journal of Mechanical and Industrial Engineering. All rights reserved

Keywords: Cutting Force, Oil Palm, Mechanized Harvesting Tool, Reciprocal Saw, Automation in Harvesting.

* Corresponding author e-mail: mikhwanr@usm.my.

1. Introduction

The oil palm (*Elaeis guineensis*), native to West Africa, has been cultivated for thousands of years and is now grown in 43 countries, with Malaysia among the largest producers [1]. In 2016, Malaysia's oil palm sector employed over 429,351 field workers [2], and by 2018, plantations covered 5.85 million hectares [3]. Despite industry growth, harvesting still relies on manual tools like sickles and chisels [4], requiring significant hand forces and repetitive motions that lead to fatigue and work-related musculoskeletal disorders (WMSDs) [5-8].

To improve ergonomics and productivity, research has focused on mechanization and automation [9, 10]. These developments are critical for the future integration of robotic systems and drone-based platforms in plantation harvesting operations, where precision cutting and minimal operator strain are key requirements. Traditional sickles and chisels, with narrow wedge angles, create high friction forces, demanding greater pulling effort during cutting. Mechanized tools, such as reciprocal electric saws or chainsaws with wider wedge angles, reduce resistance and improve cutting efficiency [11-15]. Smart technologies, like IoT-equipped drones, further optimize plantation management [14].

Research on reciprocal electric saws in oil palm harvesting is limited, especially in analysing how blade geometry, cutting angles, and feed rates affect efficiency. While circular saws have been studied for cutting power models [16], their shape is unsuitable for fronds and fresh fruit bunches (FFBs). Machines like CANTAS™ and Ckat™ improve productivity but are heavy (5-7.6 kg) and have limited reach (up to 7 meters) [4, 12, 17]. Electric saws, in contrast, offer lower emissions, reduced fuel consumption, and better ergonomics.

A key advantage of the reciprocal electric saw is that it functions as a material removal tool, eliminating the need for higher pulling force to cut through the oil palm frond. Wider wedge angles enhance penetration, improving cutting efficiency, especially for thick fronds [18]. Optimizing parameters like feed rate, frond cutting angle, and blade geometry is crucial for better performance and reduced fatigue. Cutting force is linked to tool and motion parameters [19], emphasizing the need for optimization.

This study explores the reciprocal electric saw for oil palm frond harvesting with two objectives: analysing cutting force at varying feed rates and angles and evaluating blade parameters for efficiency. The findings aim to support not only ergonomic improvements for manual and semi-mechanised harvesting, but also to inform the design of automated cutting systems, potentially integrated into robotic arms or drone-based platforms for fully autonomous harvesting applications. By optimizing these factors, the research contributes to agricultural mechanisation and engineering, with broader applications in automated cutting tools.

2. Materials and Methods

2.1. Apparatus and Material

This study used a cordless electric reciprocal saw (WORX WG894E) to investigate cutting forces in oil palm harvesting. The saw operates at 2200 rpm, outputting 45-55W (25V-28V, 1.3A-1.6A). A 3-axis load cell (MLD66, 300N capacity, 80 Hz sampling rate) measured cutting forces. A custom-designed adjustable clamp held fronds at various cutting angles. A height-adjustable jack and Ball Screw Actuator (HANPOSE® 23HS10028, 260N.cm) enabled precise linear feeding, controlled by a micro step driver (HPD970) and an Arduino Uno microcontroller.

Fresh oil palm fronds (40 cm long) from 10-15-year-old trees were used for consistency. Two blade types were evaluated: the original Jigsaw blade (WORX WG894E) with a positive rake angle and a heavy-duty pruning saw with a negative rake angle, providing a comprehensive performance evaluation.

2.2. Experimental Setup

The laboratory experiment was conducted at the Vibration Lab, School of Mechanical Engineering, Universiti Sains Malaysia. A custom jig, designed in SolidWorks (2023) and fabricated from welded iron plates and hinges, allowed adjustment to specific frond cutting angles (0°, 15°, 30°, 45°, and 60°) [20, 21]. These angles represent various cutting scenarios in oil palm harvesting. Holes drilled into the jig enabled frond locking at precise angles, verified using a protractor ruler.

An automatic feeding system controlled cutting feed rates of 5 mm/s, 10 mm/s, and 15 mm/s using a ball screw actuator and an Arduino Uno microcontroller [16]. The electric reciprocal saw was mounted on the actuator's worktable (Figure 1 (a)), with the cutting direction parallel to the x-axis of a 3-axis load cell as shown in Figure 1 (b). The load cell, positioned between the saw and worktable (Figure 1 (c)), was calibrated using known masses.

The relative blade angle was set at a 30°, angle to the x-axis of the load cell, aligning with the frond's cross-section as shown in Figure 2. This angle was influenced by the saw's body design. A purchased heavy-duty pruning saw was modified to fit the jigsaw blade adapter. The designs and parameters of both blades are shown in Figure 3 and detailed in Table 1. This setup ensured precise control, allowing systematic analysis of the effects of frond cutting angle, feed rate, and blade type on cutting forces.

The jigsaw and heavy-duty blades were selected due to their contrasting geometries and cutting profiles. The jigsaw blade with positive rake angle and finer teeth, is typically used for precision cutting, while the heavy-duty blade's larger wedge angle and negative rake angle make it suitable for high-volume material removal [15].

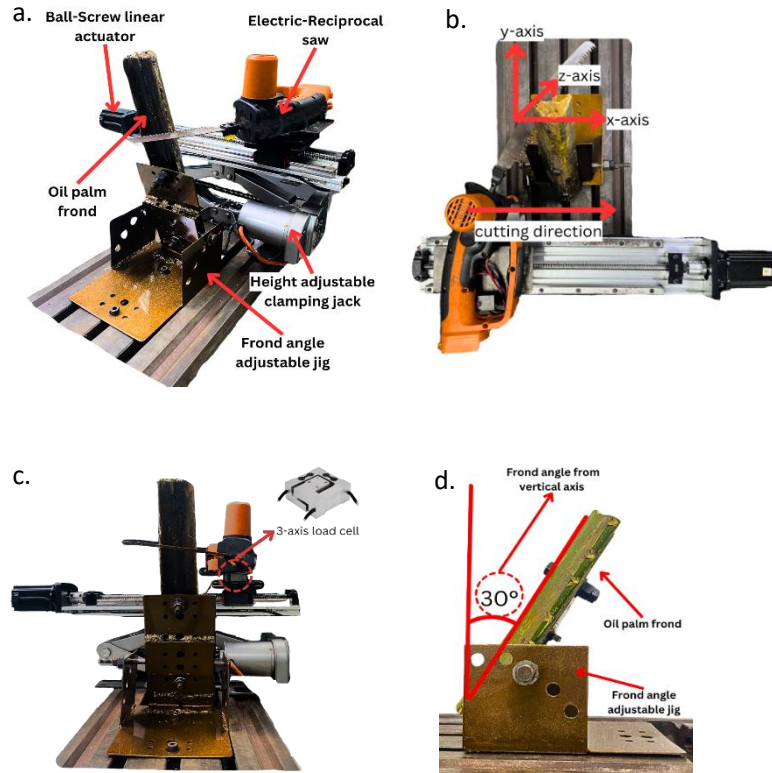


Figure 1. (a) Isometric view of overall setup, (b) the top view, (c) the front view and (d) side view relative frond cutting angle orientation.

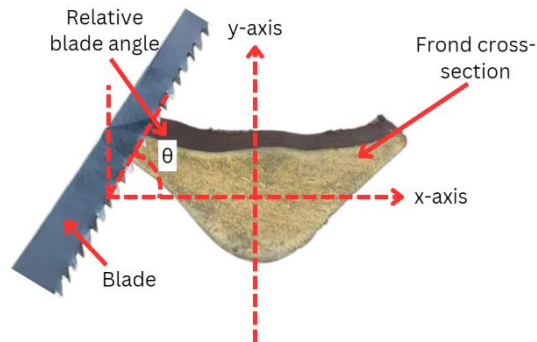


Figure 2. Schematic representation of the blade's relative angle (θ) against the x-axis of the frond cross-section along x-y load cell axis plane.

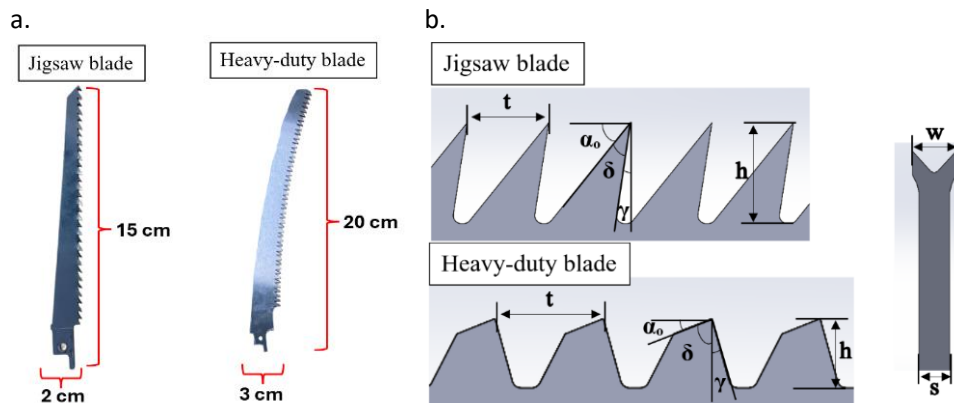


Figure 3. (a) blade design and (b) blade geometry parameters.

Table 1. Jigsaw blade and Heavy-duty bladedetailed design parameters.

Parameters	Blade types	
	A (Jigsaw blade)	B (Heavy-duty blade)
Material	High-Speed Steel	SK5 High-Carbon Steel
Features	Positive rake angle	Negative rake angle
	Withstand higher temperature	High strength and hardness
	Maintain hardness at high cutting speed	Brittle
Intended use	Wood, Plywood, Small Branches and Plastic Pipes	Tree Branches, Fruit Tree Cultivation and Garden Maintenance
Tooth pitch, t (mm)	3.80	4.70
Tooth depth, h (mm)	2.05	5.80
Cutting width, w (mm)	1.35	1.20
Blade thickness, s (mm)	1.10	1.05
Rake angle, γ (°)	+ 8.00	- 8.80
Clearance angle, α_o (°)	35.80	32.40
Wedge angle, δ (°)	48.90	57.80

2.3. Data Collection

The data collection began with the Jigsaw blade at a 0° relative frond cutting angle and a 5 mm/s feed rate. The frond was clamped securely in the jig, the feed rate set via the micro step controller, and the jack height adjusted before starting the machine.

A Vivo V9 smartphone (1080p, 30 fps) recorded the cutting process. The load cell was started to record cutting forces, while the feed rate and direction were controlled via a push button. After each cut, recordings stopped, and the cut frond was captured for thickness and surface area. Each condition was evaluated five times, using 30 fronds in total.

The procedure was then repeated for the Heavy-duty blade under identical conditions. This systematic approach ensured comprehensive data collection for analysing the effects of blade type, frond cutting angle, and feed rate on cutting forces.

2.4. Data Processing

The recorded cutting force data was processed in Python to filter noise and generate smooth data. The Savitzky-Golay filter (window size: 10, polynomial order: 3) preserved high-frequency components while reducing noise. The resultant cutting force was calculated using equation (1) [22]:

$$F_{\text{resultant}} = \sqrt{F_x^2 + F_y^2 + F_z^2} \quad (1)$$

where F_x , F_y , and F_z represent the forces measured along the x, y, and z axes, respectively.

The cutting force was normalized with respect to the volume removed per stroke (Specific Cutting Force, SCF), similarly aligned with the concept of cutting force

formulations in cutting mechanics [23]. This was calculated using the formula:

$$SCF = \frac{F_{\text{peak resultant}}}{w \times h \times \text{stroke}} \quad (2)$$

where $F_{\text{peak resultant}}$ is obtained from the equation (1), w, h and stroke represent the cutting width, tooth depth and stroke length of 16mm respectively. This normalization enabled accurate comparisons across blade types and operational parameters.

2.5. Statistical Analysis

The cutting force data were analysed using descriptive statistics, including mean and standard deviation (SD). Spearman's and Pearson's correlation coefficients were calculated in IBM SPSS to assess relationships between cutting force, feed rate, and frond cutting angle.

A t-test was conducted to compare cutting forces between the two blade types, evaluating the significance of differences due to blade design. These statistical analyses provided insights into the efficiency and effectiveness of each blade under varying conditions.

3. Results

The raw data from all three axes, along with the resultant force in both raw and smoothed forms, are shown in Figure 4. Since the frond's cutting direction was parallel to the load cell's x-axis, this axis primarily measured the direct cutting force (Figure 4a). The y-axis recorded the shearing force during forward or backward motion, while the z-axis captured upward or downward forces. Negative force values were converted to positive for clearer interpretation. The raw data was processed using the Savitzky-Golay filter to reduce noise and generate a smooth graph (Figure 4b).

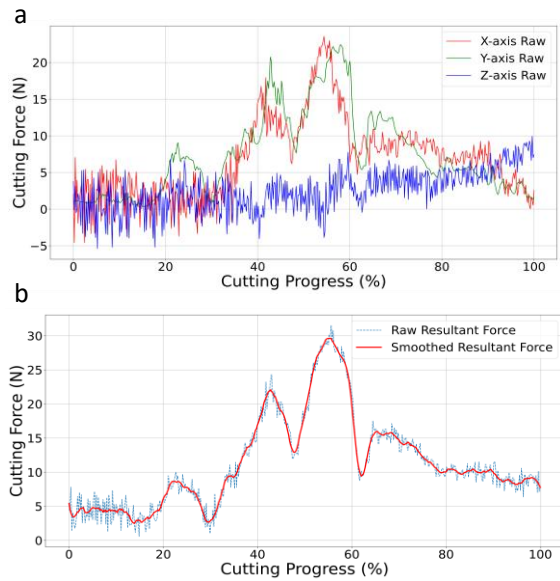


Figure 4. (a) Raw cutting force data in x-, y-, z-axis (b) raw and filtered resultant cutting force.

3.1. Peak Cutting Force vs. Frond Cross-Section (60°) (5mm/s) (2^{nd} cut).

The peak cutting force occurs at the midsection of the frond's cross-section, corresponding to time (Figure 5a), percent completion of the cut (Figure 5b), and distance (Figure 5c). The peak resultant force is recorded when the blade reaches 40%–60% of the frond's total width (Figure 5b), indicating that maximum cutting resistance occurs at the midpoint—where the cross-sectional area is largest (Figure 5c). This confirms that the highest resistance is at the frond's centre.

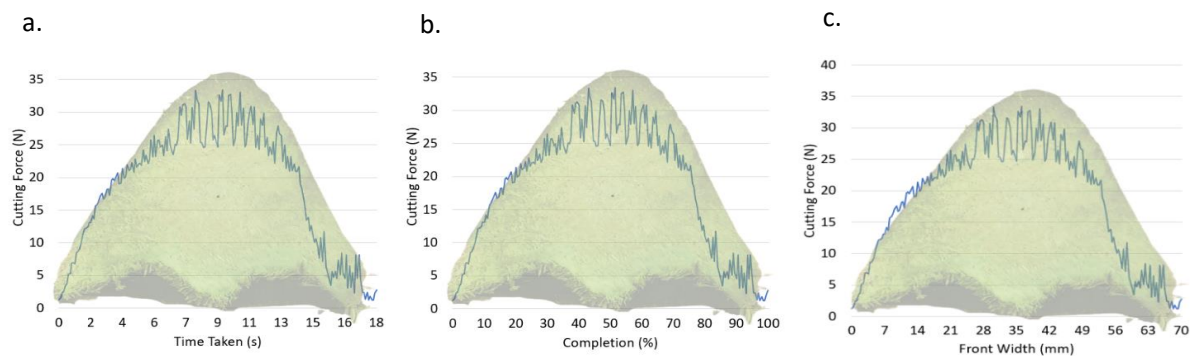


Figure 5. (a) Resultant cutting force based on time taken, (b) completion and (c) distance from 2nd trial using Jigsaw blade at relative frond cutting angle 60° , feed rate of 5mm/s .

3.2. Specific cutting force (SCF) for different feed rate, relative frond cutting angle and type of blade.

The trends in the SCF—defined as the cutting force per volume of frond removed or per stroke—reveal distinct patterns that vary with the relative frond cutting angles and feed rates for both blade types (Figure 6). At a 0° relative frond cutting angle, the jigsaw blade exhibited a sharp increase in cutting force with rising feed rates, from 0.35 N/mm^3 at 5 mm/s to 1.64 N/mm^3 at 15 mm/s . Meanwhile, the heavy-duty blade showed a more moderate rise, from 0.14 N/mm^3 to 0.69 N/mm^3 .

At 15° , the jigsaw blade maintained more consistent SCF across feed rates (0.57 N/mm^3 to 0.89 N/mm^3), while the heavy-duty blade showed a gradual increase (0.21 N/mm^3 to 0.52 N/mm^3). For 30° , the jigsaw blade's SCF rose from 0.46 N/mm^3 to 1.06 N/mm^3 , while the heavy-duty blade remained lower (0.33 N/mm^3 to 0.46 N/mm^3).

At 45° , the jigsaw blade showed a steady rise (0.57 N/mm^3 to 1.06 N/mm^3), whereas the heavy-duty blade displayed slight variability (0.31 N/mm^3 to 0.51 N/mm^3). At 60° , the jigsaw blade's SCF remained high and stable (0.67 N/mm^3 to 0.95 N/mm^3), while the heavy-duty blade showed a decline at higher feed rates (0.29 N/mm^3 to 0.25 N/mm^3).

The t-test showed significant differences in cutting forces between the two blades ($p < 0.05$). The jigsaw blade required much more force, with differences reaching 280%. At 0° and 15 mm/s , it needed 137.7% more force than the heavy-duty blade. At 15° and 5 mm/s , the difference was 171.4%, while at 30° and 10 mm/s , it was 140.5%. The largest gap appeared at 60° and 15 mm/s , where the jigsaw blade required 280% more force. These results confirm the heavy-duty blade's higher efficiency, requiring less force across all conditions.

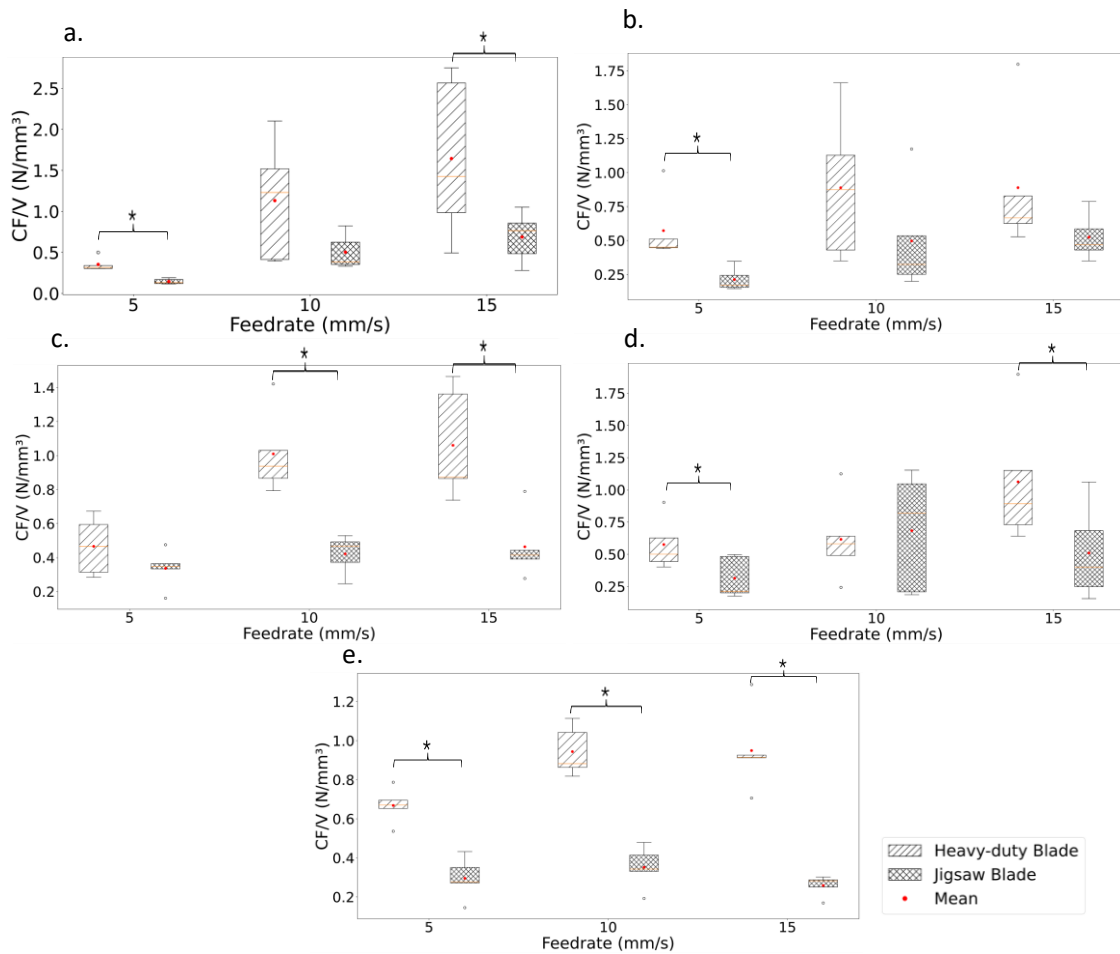


Figure 6. Box-plot for different feed rate at relative frond cutting angle of (a) 0°, (b) 15°, (c) 30°, (d) 45°, (e) 60°. *significant difference at $p < 0.05$.

Cutting efficiency, measured as frond cross-sectional area cut per second (Table 2), showed the heavy-duty blade required less time to complete a cut. For example, at 15 mm/s and 60°, the heavy-duty blade achieved 207.79 ± 57.79 mm²/s, while the jigsaw blade achieved 205.54 ± 67.79 mm²/s.

The results suggest that while both blades improve efficiency at higher feed rates and angles, the heavy-duty blade is more effective, requiring less force and cutting faster than the jigsaw blade.

3.3. 3D Relationship of Angle, Feed Rate, and SCF

The 3D graphs illustrate the relationship between SCF, relative frond cutting angle (0°–60°), and feed rate (5–15 mm/s) for both blades (Figure 7). For the jigsaw blade (Figure 7a), cutting force increases significantly with feed rate, especially at 0°, where it peaks sharply at 15 mm/s. At other angles (15°–60°), cutting force fluctuates, indicating sensitivity to feed rate changes, particularly at lower angles.

In contrast, the heavy-duty blade (Figure 7b) exhibits a more stable SCF pattern across relative frond cutting angles and feed rates. While cutting force rises gradually with higher feed rates, the trend is less pronounced, especially at higher angles. This suggests that the heavy-duty blade maintains more consistent performance, being less affected

by variations in feed rate and angle compared to the jigsaw blade, which shows greater variability.

Table 2. Mean of Frond Cross-Sectional Area per Time Taken (mm²/s)

Relative frond cutting angle (°)	Feed rate (mm/s)		
	5	10	15
Jigsaw blade			
0	114.82 ± 30.59	97.17 ± 82.30	112.52 ± 68.85
15	43.31 ± 16.49	29.08 ± 21.66	34.26 ± 16.96
30	44.97 ± 13.55	28.21 ± 22.49	36.76 ± 46.78
45	57.82 ± 10.94	45.48 ± 28.07	124.64 ± 19.64
60	97.39 ± 40.27	136.54 ± 79.36	205.54 ± 67.89
Heavy-duty blade			
0	109.14 ± 12.66	81.06 ± 45.21	47.76 ± 11.87
15	73.66 ± 26.77	80.69 ± 26.75	36.69 ± 46.58
30	34.48 ± 13.57	55.02 ± 30.19	129.02 ± 40.88
45	84.99 ± 37.47	52.80 ± 65.09	73.81 ± 46.95
60	94.54 ± 49.97	83.57 ± 69.16	207.79 ± 57.79

3.4. Correlation between SCF with feed rate and relative frond cutting angle

The analysis of cutting force, feed rate, and relative frond cutting angle reveals key differences between the jigsaw and heavy-duty blades (Table 3). For the jigsaw blade, there is a moderate positive correlation between feed rate and cutting force, indicating that higher feed rates lead to increased cutting force. This statistically significant relationship highlights the feed rate's influence on cutting performance. However, the relative frond cutting angle has little to no effect, as shown by a weak and non-significant correlation.

For the heavy-duty blade, the correlation between feed rate and cutting force is weaker but still statistically significant, suggesting that an increase in feed rate slightly raises cutting force. Like the jigsaw blade, the relative frond cutting angle has minimal impact, showing almost no correlation with cutting force. Overall, feed rate is the primary factor affecting cutting force, while relative frond cutting angle plays a negligible role for both blades.

3.5. Total length vs length at peak cutting force.

The relationship between the total length and the length at peak cutting force of the frond cross-section is analysed through two distinct plots (Figure 8). The scatter plot (Figure 8a) shows the length at peak cutting force plotted against the total frond cross-section length, with a fitted regression line. The strong positive linear relationship is indicated by a high coefficient of determination ($R^2 = 0.9233$), meaning that approximately 92.33% of the variation in the length at peak cutting force is explained by the total length. Pearson's correlation coefficient ($R = 0.9609$) further confirms this strong relationship, with a highly significant p-value (<0.00001), validating the statistical relevance at $p < 0.05$.

Additionally, the length at peak cutting force as a proportion of the total length remains consistent across different frond sizes (Figure 8b). The scatter plot shows that data points cluster closely around the mean ratio line, indicating a stable proportion regardless of total length. The Spearman's rank correlation coefficient ($R_s = 0.96072$) with a 2-tailed p-value of 0 further supports these findings, reinforcing the strong association between total length and length at peak cutting force.

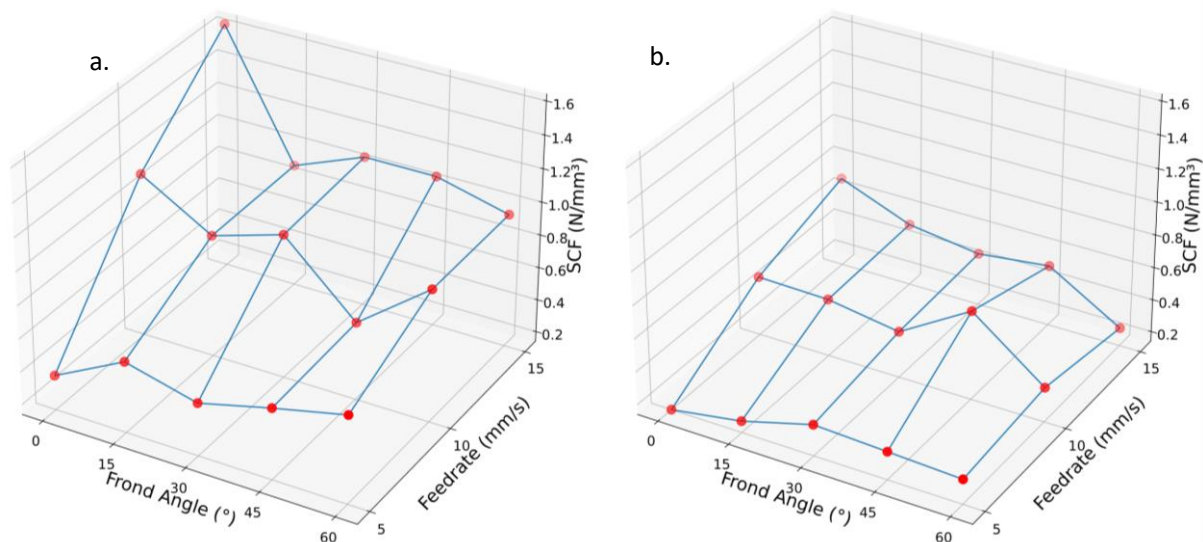


Figure 7. Relationship demonstrated in 3-dimensional (3D) between SCF with feed rate and relative frond cutting angle for (a) Jigsaw blade and (b) Heavy-duty blade.

Table 3. Correlation between SCF with feed rate and relative frond cutting angle

Specific Cutting Force (SCF)		Jigsaw blade		Heavy-duty blade	
		Feed rate	Relative frond cutting angle	Feed rate	Relative frond cutting angle
Pearson Correlation	R	0.4866	-0.1167	0.3617	-0.1082
	R^2	0.2368	0.00136	0.1308	0.0117
	p-value	0.00001	0.318721	0.00143	0.355477
Spearman's Rho (Correlation)	R_s	0.54386	0.09363	0.40696	-0.07534

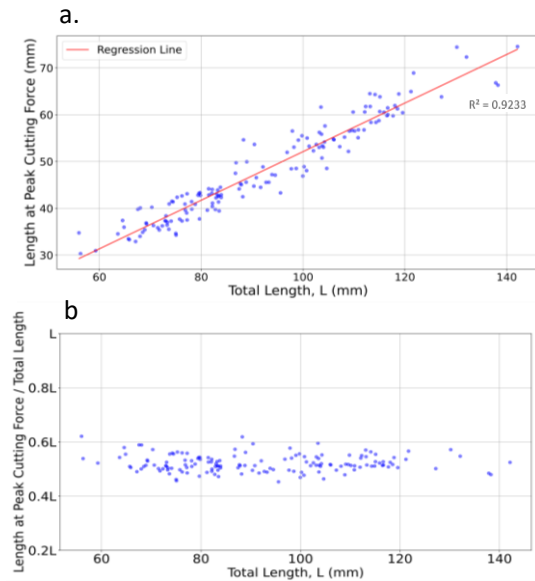


Figure 8. (a) Relationship between length at peak cutting force and (b) total length of frond cross-section and completion length and total length in term of L.

3.6. Peak resultant cutting force vs Ratio (length/thickness)

The relationship between the peak resultant cutting force and the length-to-thickness ratio of the frond cross-section is analysed in Figure 9. The scatter plot, with a dotted trend line fitted to the data, shows a weak correlation between these variables. The coefficient of determination ($R^2 = 0.0254$) indicates that only 2.54% of the variation in peak cutting force is explained by the length/thickness ratio, suggesting a minimal linear relationship.

Pearson's correlation coefficient ($R = 0.159$) further confirms this weak positive correlation. However, the p-value (0.051964) is slightly above the conventional threshold ($p < 0.05$), indicating that the result is not statistically significant. Similarly, Spearman's rank correlation coefficient ($R_s = 0.06913$) with a 2-tailed p-value of 0.40061 supports the conclusion that there is no meaningful association between these variables. Since Spearman's correlation is a non-parametric measure, it reinforces the weak and statistically insignificant relationship. These findings suggest that the absolute size of the frond (particularly thickness) rather than its aspect ratio (length/thickness) plays a more significant role in determining cutting resistance.

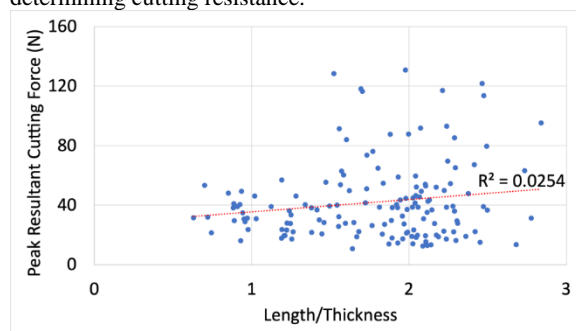


Figure 9. Peak resultant cutting force corresponding to ratio of length over thickness.

4. Discussion

This study investigates the mechanics of oil palm frond harvesting using a reciprocal electric saw, focusing on two key objectives: the effect of cutting force based on relative frond cutting angle and feed rate, and the impact of blade design on cutting force. When normalized by cutting volume per stroke, the SCF values indicate that the jigsaw blade requires more force than the heavy-duty blade, especially at higher feed rates and specific relative frond cutting angles. For example, at a 0° relative frond cutting angle, the SCF for the jigsaw blade increases significantly with rising feed rates, from 0.35 N/mm^3 at 5 mm/s to 1.64 N/mm^3 at 15 mm/s . Meanwhile, the heavy-duty blade exhibits a more moderate increase under similar conditions, with SCF values ranging from 0.14 N/mm^3 to 0.69 N/mm^3 . A similar trend is observed across other relative frond cutting angles, with the jigsaw blade requiring up to 280% more force than the heavy-duty blade at a 60° cutting angle and 15 mm/s feed rate.

These results highlight the significant impact of blade design and cutting conditions on SCF. The jigsaw blade, while effective, appears less efficient than the heavy-duty blade under certain conditions, particularly at higher feed rates and extreme cutting angles. Previous studies reported maximum SCF values for sickle and claw cutters as 1218 N/m^2 and 2290 N/m^2 , respectively [24]. A recent thesis also found that SCF decreases as the cutting angle increases, with values of $9975.38 \pm 7150.41 \text{ N/m}^2$ at 0° and $2753.74 \pm 1943.57 \text{ N/m}^2$ at 45° [21]. This study follows a similar trend, where the jigsaw blade exhibits an SCF of 1640 N/mm^3 at 0° compared to 1060 N/mm^3 at 45° . When converted to area-based SCF, this equates to 26.24 N/m^2 at 0° and 16.96 N/m^2 at 45° , supporting the thesis's findings that cutting force reduces with higher cutting angles.

Field experiment data from the same thesis showed that the maximum cutting force using the 'pelajak' sickle ($1821.60 \pm 392.03 \text{ N}$) was significantly higher than that of a conventional sickle ($1476.77 \pm 353.16 \text{ N}$) [21]. Another study reported an average cutting force of $1601.23 \pm 424.26 \text{ N}$ in field experiments [5]. In contrast, the mechanized tool used in this study demonstrated lower SCF values when normalized by volume, with peak forces much lower than those reported in field experiments. This suggests that the reciprocal electric saw could be more efficient in reducing cutting forces compared to traditional sickles used in manual harvesting.

Another notable insight observed that the peak cutting force consistently occurred at approximately 40%-60% of the frond width. This suggests a region of higher resistance due to fibre density (larger cross-sectional area), needs larger cutting force at mid-section of the frond [25 - 27]. This observation has important for the design of automated cutting systems, particularly in optimising blade entry angle, stroke timing and the strategic placement of force sensors to capture critical data during peak resistance phases. Understanding where peak force occurs can also help reduce energy consumption and improve cutting efficiency.

4.1. Effect of Relative Cutting Angle and Feed Rate on Cutting Force

The study examines the effects of feed rate and relative frond cutting angle on cutting force during oil palm frond harvesting. Results indicate that SCF increases with higher feed rates, especially at lower cutting angles. For example, at a 0° angle, SCF rises from 0.35 N/mm^3 at 5 mm/s to 1.64 N/mm^3 at 15 mm/s , aligning with previous research showing that higher feed rates require more cutting force [28]. This trend suggests that increased feed rates lead to greater material resistance, resulting in higher force demands.

Relative frond cutting angle also significantly influences SCF, with steeper angles reducing cutting force. This supports earlier studies indicating improved cutting efficiency at higher angles [20, 29]. SCF is notably lower at 45° and 60° , reflecting reduced force requirements. Statistical analysis confirms significant differences across conditions; at 0° and 15 mm/s , force demand is 137.7% higher compared to lower feed rates, while at 60° and 15 mm/s , it is 280.0% greater. These findings align with prior research emphasizing the impact of feed rate and cutting angle on cutting force [16, 30].

The study highlights the need to optimize both parameters for better efficiency. While higher feed rates increase SCF, steeper angles mitigate the effect. These insights contribute to improving harvesting strategies, confirming that both factors play a crucial role in determining cutting force. Integrating these findings into harvesting operations can enhance overall efficiency and effectiveness in oil palm frond cutting.

4.2. Effect of Blade Design and Blade Parameter Towards Cutting Force

The influence of blade design on cutting force is crucial in optimizing oil palm frond harvesting. The heavy-duty blade exhibits lower SCF than the jigsaw blade when normalized by cutting volume, making it more efficient. However, in terms of raw resultant cutting force, the heavy-duty blade requires more force in most conditions.

When comparing SCF per stroke, the heavy-duty blade demonstrates superior efficiency. For instance, at a 0° relative frond cutting angle and a 15 mm/s feed rate, the jigsaw blade's SCF is 1.64 N/mm^3 , whereas the heavy-duty blade's is significantly lower at 0.69 N/mm^3 . This trend persists across various cutting angles and feed rates, suggesting that the heavy-duty blade requires less force to remove a given volume of material. Its efficiency is attributed to design factors such as a larger wedge angle.

In contrast, the jigsaw blade demands less resultant cutting force than the heavy-duty blade, which exhibits higher force requirements due to its larger wedge angle and negative rake angle. Despite requiring more force, the heavy-duty blade cuts through a greater volume per stroke, making it more effective for substantial material removal. The jigsaw blade exerts less force but removes less material per stroke, resulting in lower cutting efficiency overall.

Statistical analysis confirms these findings, with significant differences in cutting forces between the blades. At a 0° cutting angle and 15 mm/s feed rate, the jigsaw blade's resultant force is 137.7% higher than the heavy-duty

blade's. This difference reaches 280.0% at a 60° cutting angle and 15 mm/s feed rate, reinforcing the heavy-duty blade's advantage in maintaining lower cutting forces under most conditions.

Further analysis of the 3D surface plots (Figure 7) reveals that the jigsaw blade exhibits significant SCF variability across feed rate–angle combinations. Particularly at lower angles (0° – 15°), SCF spikes sharply with increasing feed rate, reflecting inconsistent material engagement. This instability may be attributed to its geometry which leads to increased friction, tearing of fibrous tissue, and reduced chip evacuation efficiency. In contrast, the heavy-duty blade shows a more stable SCF profile across all cutting conditions. Although it requires higher resultant cutting forces due to its negative rake angle and larger wedge angle. These features promote a more efficient shearing mechanism and enable more material to be removed per stroke. As a result, the heavy-duty blade achieves lower SCF values even under increased feed rates and steeper cutting angles.

Blade parameters like rake and wedge angles play a key role in cutting performance. The jigsaw blade's positive rake angle ($+8.00^\circ$) helps reduce SCF and resultant force compared to the heavy-duty blade's negative rake angle (-8.80°). Additionally, the heavy-duty blade's larger wedge angle (57.80° vs. 48.90° for the jigsaw blade) contributes to higher cutting forces, aligning with studies showing that increased wedge angles lead to higher force requirements but improved efficiency in specific applications [31–34]. While the heavy-duty blade has a thinner profile that should reduce friction, its large wedge angle and negative rake increase resistance. However, because it removes a greater volume per stroke due to deeper teeth and a narrower kerf, its SCF remains lower, making it more efficient.

Overall, the heavy-duty blade's lower SCF, particularly at higher feed rates and steeper cutting angles, makes it more suitable for high demand cutting conditions. Meanwhile, the jigsaw blade, despite its higher SCF, performs consistently across different conditions. Understanding the influence of wedge and rake angles is essential for optimizing blade design and improving cutting efficiency in harvesting applications.

4.3. Cutting Time

The results from Table 2 indicate that both feed rate and relative frond cutting angle significantly influence the time required to cut oil palm fronds. Higher feed rates enhance cutting efficiency for both blades, though the effect varies with the cutting angle. This finding aligns with prior research emphasizing the need to optimize feed rates, such as 10 mm/s , to balance efficiency and energy consumption in mechanized cutting tools [16].

For the jigsaw blade, cutting efficiency decreases at mid-range angles (15° to 30°), particularly at lower feed rates. However, at extreme angles and higher feed rates, it performs more effectively. The highest efficiency is observed at 60° and 15 mm/s , reaching a peak value of $205.54 \text{ mm}^2/\text{s}$. Similarly, the heavy-duty blade exhibits its best performance at 60° and 15 mm/s , with a peak efficiency of $207.79 \text{ mm}^2/\text{s}$. However, it experiences a significant drop in efficiency at 0° and 15 mm/s , suggesting challenges in

maintaining consistent cutting performance under these conditions.

The variability observed, particularly in the mid-range angles, suggests that factors such as frond material properties and blade dynamics play a crucial role in the cutting process. While both blades improve in efficiency at higher feed rates and extreme angles, the jigsaw blade demonstrates a more pronounced gain at 60°, especially at the highest feed rate evaluated. This highlights the importance of optimizing blade selection and cutting parameters to maximize harvesting efficiency.

4.4. Correlation Analysis

The correlation analysis reveals that the relationship between specific cutting force (SCF) and feed rate is stronger for the jigsaw blade than for the heavy-duty blade. Both Pearson and Spearman correlation analyses were used to evaluate relationship between SCF and cutting parameters. The Pearson correlation coefficient (R) for the jigsaw blade is 0.4866, whereas for the heavy-duty blade, it is 0.3617. This suggests that as the feed rate increases, SCF rises more noticeably for the jigsaw blade. In contrast, the heavy-duty blade exhibits a more consistent SCF across varying feed rates, indicating that feed rate has a less significant impact on SCF for this blade. This stability highlights the heavy-duty blade's ability to maintain cutting efficiency regardless of feed rate fluctuations.

The weak correlation can be attributed to the behaviour of SCF across different relative frond cutting angles. As the angle increases from 0° to 30°, SCF tends to rise due to the blade encountering fibres in a more perpendicular orientation, which increases resistance. However, beyond 45° to 60°, SCF decreases as the fibres align more with the cutting direction, reducing resistance and improving cutting efficiency. This non-linear trend explains why the correlation between SCF, and feed rate is weak overall—it is influenced by the complex interplay between relative frond cutting angle and fibre orientation rather than feed rate alone. While Pearson's values confirmed linear trends, Spearman's coefficients further validated these associations by capturing monotonic but potentially non-linear relationships, enhancing the robustness of the analysis.

4.5. Strength and limitations of the study

The findings of this study contribute to the development of automated harvesting systems, including drones and robotic machinery. Understanding optimal cutting parameters enables precise, efficient cuts, enhancing worker safety while improving productivity. These insights support the design of drones with cutting mechanisms and autonomous harvesting robots.

By optimizing feed rate, frond cutting angle, and blade type, this study enhances reciprocal electric saw performance and advances mechanized harvesting. However, limitations exist controlled conditions may not reflect real-world variability, findings apply specifically to reciprocal electric saws, and long-term durability was not assessed.

Future research should validate results in field conditions, explore alternative cutting technologies, and

assess tool longevity. Addressing these aspects will help develop practical, sustainable solutions for oil palm harvesting.

5. Conclusion

This study provides significant contributions to the mechanisation of oil palm harvesting by analysing cutting force under varying feed rate, relative frond cutting angle, and blade design. The findings clearly demonstrate the superiority of the heavy-duty blade, which consistently exhibit lower SCF—137.7% to 280% lower than the jigsaw blade—affirming for efficient frond cutting. SCF for the jigsaw blade rises significantly with feed rate, while the heavy-duty blade maintains stable performance. Additionally, variations in cutting angle reveal important insights, increasing from 0° to 30° due to resistance and decreasing from 45° to 60° as fibre alignment improves cutting efficiency.

These results not only advance understanding of cutting dynamics in fibrous biomaterials but also provide a foundational reference for the development of more effective and ergonomic harvesting tools. They directly support the design of autonomous or semi-autonomous harvesting system aimed at reducing human labour and improving productivity. Moreover, the insights gained are applicable to other fibrous crops such as sugarcane and banana, expanding the study's relevance across the agricultural sector.

Future research should include field-based validation under real plantation conditions, long-term performance and wear analysis of blade types and integration of SCF trends into development of autonomous harvesting systems.

CRediT authorship contribution statement

Umesh Ganesh: Methodology, Analysis, Investigation, Writing-Original draft preparation. Zaidi Mohd Ripin: Supervision, Conceptualization, Methodology, Writing-review, and editing. Wan Mohd Amri Wan Mamat Ali: Conceptualization, Methodology, Resources. Mohamad Ikhwan Zaini Ridzwan: Visualization, Project administration, Conceptualization, Methodology, Writing-review, and editing.

Acknowledgement

The author would like to express special thanks to Universiti Sains Malaysia for the financial assistance provided through the Bridging Grant (R501-LR-RND003-0000000557-0000). The author also acknowledges the use of artificial intelligence tools, including OpenAI's ChatGPT, for assistance in structuring, grammar checking, and language refinement of this manuscript.

Declaration of competing interest

The author declares that they have no known competing financial interests or personal relationships that could have appeared to influence the work reported in this paper.

References

- [1] G.K.A. Parveez, A.H.A. Tarmizi, S. Sundram, S.K. Loh, M. Ong-Abdullah, K.D.P. Palam, K.M. Salleh, S.M. Ishak, Z. Idris, "Oil palm economic performance in Malaysia and R&D progress in 2020", *J. Oil Palm Res.*, vol. 33, no. 2, 2021, pp. 181–214. <https://doi.org/10.21894/jopr.2021.0026>.
- [2] K.H.D. Tang, H.M.S. Al Qahtani, "Sustainability of oil palm plantations in Malaysia", *Environ. Dev. Sustain.*, vol. 22, no. 6, 2020, pp. 999–5023. <https://doi.org/10.1007/s10668-019-00458-6>.
- [3] A.R. Shuib, M.K.F.M. Radzi, M.A.M. Bakri, M.R.M. Khalid, "Development of a harvesting and transportation machine for oil palm plantations", *J. Saudi Soc. Agric. Sci.*, vol. 19, no. 5, 2020, pp. 365–373. <https://doi.org/10.1016/j.jssas.2020.05.001>.
- [4] A. Oyediji, A. Umar, L. Kuburi, I. Apeh, "Trend of Harvesting of Oil Palm Fruit; The Mechanisms, and Challenges", *IJSER*, vol. 3, no. 3, 2020, pp. 2581–7175.
- [5] N.A. Abdullah, M.N. Mohamad Shaberi, M.N.A. Nordin, Z. Mohd Ripin, M.F. Razali, W.M.A. Wan Mamat Ali, B. Awang, M.I.Z. Ridzwan, "Field measurement of hand forces of palm oil harvesters and evaluating the risk of work-related musculoskeletal disorders (WMSDs) through biomechanical analysis", *Int. J. Ind. Ergonom.*, vol. 96, no. 10, 2023, pp. 110–115. <https://doi.org/10.1016/j.ergon.2023.103468>.
- [6] M.I.H. Azaman, A.S. Ramli, M.K.F. Mdradzi, M.R. Ahmad, M.R.M. Khalid, M.A.M. Bakri, Y.M. Kamil, M.A. Mahdi, "Feasibility Study of Oil Palm Harvesting Using Pulse Fibre Laser System with Different Lenses", *J. Oil Palm Res.*, vol. 34, no. 3, 2022, pp. 488–496. <https://doi.org/10.21894/jopr.2022.0005>.
- [7] M. Mokhtar, B. Deros, E. Sukadarin, "Evaluation of musculoskeletal disorders prevalence during oil palm fresh fruit bunches harvesting using RULA", *Adv. Eng. Forum.*, vol. 10, 2013, pp. 110–115. <https://doi.org/10.4028/www.scientific.net/AEF.10.110>.
- [8] E.H. Sukadarin, B. Md Deros, J.A. Ghani, A.R. Ismail, M.M. Mokhtar, "Investigation of Ergonomics Risk Factors for Musculoskeletal Disorders among Oil Palm Workers Using Quick Exposure Check (QEC)", *Adv. Eng. Forum.*, vol. 10, 2013, pp. 103–109. <https://doi.org/10.4028/www.scientific.net/AEF.10.103>.
- [9] R.A. Aljawadi, D. Ahmad, N. Mat-Nawi, M. Saufi, "Mechanized harvesting of oil palm fresh fruit bunches: A review", in *Proc. Conf. Capacity Building in Agriculture, Forestry and Plantation, Bangi*, 2018.
- [10] A. Oyediji, A. Umar, L. Kuburi, A. Edet, Y. Mukhtar, "Development and performance evaluation of an oil palm harvesting robot for the elimination of ergonomic risks associated with oil palm harvesting", *J. Agric. Eng.*, vol. 53, no. 3, 2022, pp. 1388. <https://doi.org/10.4081/jae.2022.1388>.
- [11] A. Hamsi, T.B. Sitorus, T.B. Isma, "Design assembling and testing of the oil palm bunches cutting machines", *Mater. Sci. Eng.*, vol. 1003, no. 1, 2020, 012016. <https://doi.org/10.1088/1757-899X/1003/1/012016>.
- [12] A.R. Jelani, "Development and evaluation of a new generation oil palm motorised cutter (Cantas Evo)", *J. Oil Palm Res.*, 2018. <https://doi.org/10.21894/jopr.2017.0000>.
- [13] A.R. Jelani, A. Hitam, J. Jamak, M. Noor, Y. Gono, O. Ariffin, "Cantas™—A Tool For The Efficient Harvesting Of Oil Palm Fresh Fruit Bunches", *J. Oil Palm Res.*, vol. 20, 2008, pp. 548–558.
- [14] Z. Khuzaimah, N.M. Nawi, S.N. Adam, B. Kalantar, O.J. Emeka, N. Ueda, "Application and Potential of Drone Technology in Oil Palm Plantation: Potential and Limitations", *J. Sens.*, vol. 2022, no. 1, 2022. <https://doi.org/10.1155/2022/5385505>.
- [15] U. Ganesh, Z.M. Ripin, W.M.A.W.M. Ali, Y.Y. Heng, M.J.J. Law, J. Karunakaran, M.I.Z. Ridzwan, "A Biomechanical Analysis on Work-Related Musculoskeletal Disorders Using A Mechanised Chainsaw For Oil Palm Harvesting", *J. Oil Palm Res.*, 2024. <https://doi.org/10.21894/jopr.2024.0045>.
- [16] S. Qun, M.Z. Ripin, "Analysis Of The Energy Consumption Of Motorised Circular Saw When Cutting Oil Palm Frond", *J. Oil Palm Res.*, 2023a. <https://doi.org/10.21894/jopr.2023.0063>.
- [17] I.V.S. Reddy, "Status And Need Of Mechanization Of Oil Palm Harvesting In Telangana", *AMA*, vol. 53, no. 4, 2022, pp. 7389–7394. <https://doi.org/10.6084/m9.figshare.19672278>.
- [18] P.R. Anilkumar, B. Aroli Rahul, P.V. Gowda Shyam, D. Tejas, K. Tharun, "Design and Fabrication of Electric Portable Tiller for Agricultural Purpose", *IJASRE.*, vol. 9, no. 5, 2023, pp. 48–54. <https://doi.org/10.31695/IJASRE>.
- [19] Y. Gao, X. Hu, S. Tong, J. Kan, Y. Wang, F. Kang, "Multi-objective Optimization of Peak Cutting Force and Cutting Energy Consumption in Cutting of Caragana korshinskii Branches", *BioResources.*, vol. 17, no. 4, 2022, pp. 6325–6340. <https://doi.org/10.15376/biores.17.4.6325-6340>.
- [20] M.R. Ahmad, N. Jamaludin, A.R. Jelani, A. Bakri, A.R. Shuib, "The Effect of Design Parameters on The Force And Energy Requirement For Cutting Oil Palm Fronds using Magnetic Force", *J. Teknol.*, vol. 82, no. 4, 2020. <https://doi.org/10.11113/jt.v82.14236>.
- [21] A.H.B.A.M. Muhammad, "Analysis of Design of an Intervention Oil Palm Sickle", *B.Eng. Thesis, Universiti Sains Malaysia*, 2022.
- [22] M.S. Kasim, M.S.N. Salleh, N.M. Yusof, M.Z. Ramli, I. Mohamad, "Prediction of Cutting Force in End Milling of Inconel 718", *J. Mech. Eng. Sci.*, vol. 8, 2015, pp. 1351–1360.
- [23] T. Zhang, Z. Liu, C. Xu, "Theoretical Modeling and Experimental Validation of Specific Cutting Force for Micro End Milling", *Int. J. Adv. Manuf. Technol.*, vol. 77, no. 5–8, 2015, pp. 1433–1441. <https://doi.org/10.1007/s00170-014-6549-1>.
- [24] A.R. Jelani, D. Ahmad, A. Yahya, "Force and energy requirement for cutting oil palm fronds", *J. Oil Palm Res.*, vol. 10, 1998, pp. 10–24.
- [25] K. Gokul, T. Rajasekaran, "Cutting force analysis on drilling parameters of sugarcane fibre reinforced polymer composite", *IOP Conference Series: Materials Science and Engineering*, Vol. 402, 2018, Article ID 012183. <https://doi.org/10.1088/1757-899X/402/1/012183>.
- [26] A. Kakitis, U. Bērziņš, R. Berzins, R. Brencis, "Cutting properties of hemp fibre", 2012. [Online]. Available: <https://consensus.app/papers/cutting-properties-of-hemp-fibre-berzins-brencis/fed88af8c4db508a93445a82eae247f7/>
- [27] M. El Messiry, A. Eloufy, S. Latif, E. Eid, "Evaluation of cutting force of high-performance fibers' dynamic cutting behaviour", *Journal of Industrial Textiles*, Vol. 51, 2021, pp. 3393–3412. <https://doi.org/10.1177/1528083721990752>
- [28] M.J. Mir, M.F. Wani, "The influence of cutting fluid conditions and machining parameters on cutting performance and wear mechanism of coated carbide tools", *JTrib.*, vol. 18, 2018.
- [29] A.R. Jelani, *Design And Development Of An Oil Palm Fresh Fruit Bunch Cutting Device*, 1997.
- [30] S. Qun, Z.M. Ripin, "Modeling Of Cutting Force For Palm Oil Fronds", *Eng. Agric.*, vol. 43, no. 4, 2023b. <https://doi.org/10.1590/1809-4430-Eng.Agric.v43n4e20230081/2023>.
- [31] D. Yang, X. Wang, Y. Wang, H. An, Z. Lei, "Experiment and Analysis of Wedge Cutting Angle on Cutting Effect", *Adv. Civ. Eng.*, vol. 2020, no. 4, 2020, pp. 1–16. <https://doi.org/10.1155/2020/5126790>.
- [32] S. Kaneko, S. Nagasawa, "Wedge indentation characteristics of pressure-sensitive adhesives sandwiched by polyethylene

- terephthalate films", JAMDSM., vol. 14, no. 1, 2020, pp. 1–18. <https://doi.org/10.1299/jamdsm.2020jamdsm0007>.
- [33] S. Sulaiman, A. Roshan, M.K.A. Ariffin, "Finite Element Modelling of the effect of tool rake angle on tool temperature and cutting force during high speed machining of AISI 4340 steel", IOP Conf. Ser. Mater. Sci. Eng., vol. 50, no. 1, 2013. <https://doi.org/10.1088/1757-899X/50/1/012040>.
- [34] H. Yanda, J.A. Ghani, C. Hassan, C. Haron, "Effect of Rake Angle on Stress, Strain and Temperature on the Edge of Carbide Cutting Tool in Orthogonal Cutting Using FEM Simulation", Eng. Sci., vol. 42, no. 2, 2010. <https://doi.org/10.5614/itbj.eng.sci.2010.42.2.6>.